JCTC Journal of Chemical Theory and Computation

Article

pubs.acs.org/JCTC

Charge Transfer Models of Zinc and Magnesium in Water

Marielle Soniat,[†] Lisa Hartman,[‡] and Steven W. Rick*[,†]

[†]Department of Chemistry, University of New Orleans, New Orleans, Louisiana 70148, United States

[‡]Benjamin Franklin High School, New Orleans, Louisiana 70122, United States

Supporting Information

ABSTRACT: Quantum mechanical studies point to the importance of polarization and charge transfer (CT) in zinc binding. A new CT force field is used to study these effects in ion−water dimers and in aqueous solution. Quantum mechanics calculations are carried out to determine amounts of CT. Models for zinc and magnesium are parametrized to reproduce solvation structure, hydration free energy, and CT properties. The new models are subjected to energy decomposition, in which the effects of polarization and CT are investigated. The importance of these multibody interactions in the liquid is also considered. We find that, for divalent cations, polarization and charge transfer both strongly affect binding to water. Though polarization increases the internal (self) energy of water and ions, this is more than compensated for by a stronger ion−water interaction energy. The direction of the charge transfer from the water to the cation weakens the ion−water interaction; this increase in energy is counteracted by a decrease in the system energy due to electron delocalization.

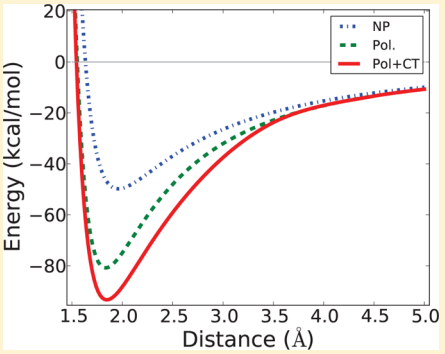

INTRODUCTION

The assessment of various components of intermolecular interactions is important in the understanding of molecular association and in the development of molecular mechanics models. It is illustrative to consider intermolecular interactions based on the electronic response induced by other molecules. If the electronic distribution is strongly influenced by the presence of another molecule, then polarizability will give rise to nonpairwise additive effects. Electron density can be shifted between particles, resulting in charge transfer (CT). Recent models have been developed that incorporate CT into a classical molecular mechanics force field.[1,2]

Let us consider an example system of a cation−water dimer. From a quantum mechanics (QM) perspective, the electron clouds of the ion and water shift in response to the electric field generated by the other species, resulting in mutual polarization. Additionally, the electrons are delocalized over the total system. If the electron density is partitioned, using Bader's atoms-in-molecules (AIM) method for example,[3] the electron density of the water molecule has some probability to be found on the cation. This charge transfer thus results in a water molecule that is on average positively charged, and a cation that has a charge value that is reduced from its formal charge.

The charge transfer force field (FF) captures CT by recalculating the charge of every species at each time step. Although the charge is conserved in the total system, the charge of each species is based on its local coordination structure and changes as the solvation structure is altered.[4] Use of a FF allows us to study the effects of CT on longer time scales and larger system sizes than are accessible by QM. This CT force field has allowed us to study charge distributions in aqueous solutions[2] and the surface charge of water.[4,5]

Systems that include zinc are suspected to be strongly influenced by CT.[6] Traditional (fixed charge) models of zinc are inadequate for studies of zinc partitioning between water and protein binding sites.[7] Polarization is known to contribute strongly to the energetics of zinc binding.[7] Additionally, QM studies show CT on zinc in these binding sites.[6,8] For thermodynamic studies, models of bound zinc have been introduced. These models have a reduced zinc charge (i.e., $q(\mathrm{Zn}) < +2e$) and are covalently bound via strong harmonic restraints to the binding site.[9] Although these models improve the overall description of the protein, they obviously cannot capture the movement of zinc into and out of the binding site. Incorporating polarizability and CT may provide a model of zinc that is accurate in both the hydrated and protein-bound state. As a first step toward this type of model, herein we parametrize zinc−water interactions in a polarizable and charge transfer FF.

For comparison, we also parametrize another divalent cation, magnesium. Magnesium provides an interesting comparison because it has the same hydration number, 6,[10] and a similar size as zinc. The ion−water dimer interaction for Zn^{2+} is 20 kcal mol^{-1} stronger than for Mg^{2+}.[11−13] Assuming that the entropic contributions are similar, Zn^{2+} should have a free energy of hydration that is 120 kcal mol^{-1} more favorable. And yet, the hydration free energy for Zn^{2+} is only ∼30 kcal mol^{-1} more negative than for Mg^{2+},[14] suggesting that there are important nonadditive interactions. In general, divalent ions can be expected to show larger nonadditive effects, both in terms of polarizability and CT, than monovalent ions.

Received: December 22, 2014
Published: February 20, 2015

DOI: 10.1021/ct501173n
J. Chem. Theory Comput. 2015, 11, 1658−1667

The extent to which CT alters energetics and its importance relative to polarization have been explored in a number of energy decomposition schemes.[15−22] However, they tend to disagree on the amount of both CT and energy contributed per electron transferred. Using our force field model, we explore the interaction of CT and polarization using energy decomposition analysis (EDA). We base our EDA on the simple and intuitive method of Kitaura and Morokuma (KM),[16] as described in the Energy Decomposition section below.

We find that CT plays a large role in ion−water binding for divalent cations. CT acts through an explicit CT energy (U_{CT}) and by altering the charge distribution in the system. For monovalent ions, the main contribution of CT is through altering ion−water induced electrostatics in which U_{CT} plays only a minor role.

METHODS

When developing molecular mechanics force fields, a variety of parameters need to be set at particular values. Although the values of the parameters are not necessarily unique, careful choice of parameters will allow for more accurate simulations. Our general approach to parametrization involves quantum chemical calculation of charge transfer amounts, determination of polarizability (usually available in the literature), calculation of the ion−water dimer potential energy surface, and simulation of a single ion in bulk water. CT and polarizability parameters are set based on quantum mechanical data. The remaining (five) parameters are adjusted freely to get the best agreement with dimer and aqueous properties known from experimentation and high-level quantum calculations. This adjustment can be done manually or using an automated optimization procedure. Finally, the quality of the parameters is confirmed by calculating single-ion solvation free energy.

Quantum Chemistry Calculations. The geometry of ion−water dimers is optimized using the meta-generalized gradient approximate (meta-GGA) density functional of Tao, Perdew, Staroverov, and Scuseria (TPSS)[23] in Gaussian 09.[24] TPSS with Grimme's dispersion correction (D3) and Becke−Johnson damping[25] is also tested. Because of the large memory requirements of meta-GGA, PBEPBE GGA[26,27] is used for larger clusters. Several basis sets and effective core potentials (ECPs) are tested. For zinc, the ECP is compared to cc-pvDz for the dimer, and no significant difference in geometry or CT is found. The charge distribution is calculated using TPSS, Hartree−Fock (HF), and Møller−Plesset perturbation (MP2) theory. The electron density distribution is partitioned using AIMAll software[28] for the quantum theory of atoms in molecules (AIM).

In addition to ion−water dimers, clusters of the ions with multiple waters are also studied. Because both ions are coordinated by six waters when in bulk liquid, clusters of six waters were optimized and the charges obtained. To confirm that the second solvation shell does not alter CT within the first shell, we also studied 6 + 4, 6 + 8, and 6 + 12 clusters, where the first and second numbers are the number of waters in the first and second shells, respectively.

To simplify the tables, the letter codes shown in Table 1 are used to represent the different combinations of basis sets used in the quantum calculations.

The Model. The potential model treats polarizability for water using a fluctuating charge formalism[29] in which an atomic charge is treated as a dynamical variable, which responds to its electric field, and for an ion using a Drude, or charge on a spring model, in which the position of an additional charge site located on a harmonic spring responds to the electric field. Charge transfer is treated with the discrete charge transfer method.[1] For a discussion of that method, as well as a listing of other methods for treating CT in simulations, see ref 1. The total interaction energy, ΔE, of an ion−water pair is the sum of van der Waals dispersion, U_{vdw}, repulsion, U_{repl}, electrostatic interactions, U_{el}, polarization of the Drude particle on the ion, $\Delta U_{pol,Drude}$, polarization of the fluctuating charges on the water, $\Delta U_{pol,FQ}$, the charge transfer energy, U_{CT}, and the gas-phase energy of each monomer, E_{gp}.

Table 1. Basis Set Abbreviations

zinc basis set codes	
A	Zn cc-pvDz, O aug-cc-pvTz, H cc-pvDz
B	Zn aug-cc-pvDz, O aug-cc-pvTz, H cc-pvTz
C	Zn MDF10; O aug-cc-pvdz; H cc-pvdz
D	Zn MDF10, O 6-31G*, H 6-31G*
magnesium basis set codes	
J	Mg aug-cc-pvTz, O aug-cc-pvTz, H cc-pvTz
K	6-31G*
L	Mg cc-pvdz, H cc-pvdz, O aug-cc-pvdz

$$\Delta E = U_{vdw} + U_{repl} + U_{el} + U_{pol,Drude} + U_{pol,FQ} + U_{CT} - \sum E_{gp} \quad (1)$$

Individually,

$$U_{vdw} = -4\epsilon\left(\frac{\sigma}{r_{ij}}\right)^6 \quad (2)$$

and

$$U_{repl} = 4\epsilon\left(\frac{\sigma}{r_{ij}}\right)^{12} \quad (3)$$

where ϵ and σ are the Lennard−Jones parameters, and r_{ij} is the interparticle distance.

$$U_{el} = \sum \frac{q_i q_j}{r_{ij}} S_{ij}(r_{ij}) \quad (4)$$

where q_i and q_j are the charges, and S_{ij} is the damping function

$$S_{ij} = 1 - \left(1 + \frac{r_{ij}}{2a_{ij}}\right)e^{-r_{ij}/a_{ij}} \quad (5)$$

where a_{ij} is the Tholé damping parameter. S_{ij} prevents over polarization of the Drude particles at short-range but does not alter long-range electrostatics.

The ion interacts with its Drude particle only through x_D, the displacement of the Drude particle from the ion center, and the strength of the spring connecting them

$$U_{pol,Drude} = \frac{1}{2}k_D x_D^2 \quad (6)$$

where k_D is the spring constant and is set to 1000 kcal mol^{-1} Å^{-2} and pol indicates the polarized values. Water self-energy arises from the Coulomb overlap integral, $J_{\alpha\beta}$,

$$J_{\alpha\beta}(r_{\alpha\beta}) = \int dr_\alpha dr_\beta \left|\phi_{n_\alpha}(r_\alpha)\right|^2 \frac{1}{|r_\alpha - r_\beta - r|}\left|\phi_{n_\beta}(r_\beta)\right|^2 \quad (7)$$

DOI: 10.1021/ct501173n
J. Chem. Theory Comput. 2015, 11, 1658−1667

of Slater functions

$$\phi_\alpha(r) = A_{n_\alpha} r^{n_\alpha - 1} e^{-\zeta_\alpha r} \tag{8}$$

where A_{n_α} is a normalization constant, n_α is the principal quantum number of charge site α, and ζ_α is considered an adjustable parameter. Thus, the water self-term is

$$U_{\mathrm{pol,FQ}} = \sum_\alpha \tilde{\chi}_\alpha^0 q_\alpha + \frac{1}{2}\sum_\alpha \sum_\beta q_\alpha q_\beta J_{\alpha\beta}(r_{\alpha\beta}) \tag{9}$$

where $\tilde{\chi}_\alpha^0$ is the Mulliken electronegativity of the α atom.

The transfer of electron density from one molecule to another introduces an additional stabilization modeled by

$$U_{\mathrm{CT}} = -\mu_{ij}^{\mathrm{CT}} |q_{ij}^{\mathrm{CT}}| + \frac{1}{2}\eta_{ij}^{\mathrm{CT}} (q_{ij}^{\mathrm{CT}})^2 \tag{10}$$

where μ_{ij}^{CT} and η_{ij}^{CT} represent the electronegativity and hardness for CT, respectively. The amount of charge transferred, q_{ij}^{CT}, is given by

$$q_{ij}^{\mathrm{CT}} = \begin{cases} Q_{ij}^{\mathrm{CT}}, \text{ if } r_{ij} < R_1^{\mathrm{CT}} \\ \dfrac{1}{2} Q_{ij}^{\mathrm{CT}} \left[1 + \cos\left(\pi \dfrac{r_{ij} - R_1^{\mathrm{CT}}}{R_2^{\mathrm{CT}} - R_1^{\mathrm{CT}}} \right) \right], \\ \quad \text{if } R_1^{\mathrm{CT}} \le r_{ij} \le R_2^{\mathrm{CT}} \\ 0, \text{ if } r_{ij} > R_2^{\mathrm{CT}} \end{cases} \tag{11}$$

where Q_{ij}^{CT} is the maximum amount of CT for each pair and depends on the pair type. The distances R_1^{CT} and R_2^{CT} define where the switching function starts and ends, respectively, for each pair type.

Lastly, E_{gp} is the gas-phase energy of each (isolated) monomer. For ions, $E_{\mathrm{gp}} = U_{\mathrm{gp,Drude}}$, where $U_{\mathrm{gp,Drude}}$ has the same definition as eq 6 except it uses the unpolarized Drude displacement. Because $x_{\mathrm{D}} = 0$ for a nonpolarized ion, $E_{\mathrm{gp}} = 0$. For water, $E_{\mathrm{gp}} = U_{\mathrm{gp,FQ}}$, where $U_{\mathrm{gp,FQ}}$ has the same definition as eq 9, but gp indicates using the gas-phase (nonpolarized) values for charges. $\Delta U_{\mathrm{pol,FQ}}$ refers to the difference in polarized and gas-phase water self-energy.

Note that U_{vdw}, U_{repl}, U_{el}, and U_{CT} are intermolecular terms (denoted by ij), whereas $U_{\mathrm{pol,Drude}}$ and $U_{\mathrm{pol,FQ}}$ are intramolecular (denoted by $\alpha\beta$). The intermolecular interactions can alter the intramolecular interactions, and vice versa, if polarization is allowed. As described above, the parameters Q_{ij}^{CT}, R_1^{CT}, R_2^{CT}, q_{D}, and k_{D} are set with the QM data. For Zn^{2+} and Mg^{2+}, the CT parameters are based on the six-water clusters. The remaining parameters, ϵ, σ, a_{ij}, μ_{ij}^{CT}, and η_{ij}^{CT}, are adjusted to get ion−water dimer and aqueous single-ion properties in agreement with experiment and ab initio molecular dynamics.

Energy Decomposition. The roles of polarization and CT in ion−water interactions are explored by energy decomposition analysis (EDA). The process is similar to the Kitaura−Morokuma (KM) method.[16] The definition of our terms are slightly different in that our binding energies contain repulsion (U_{repl}) and dispersion (U_{vdw}), which are separate in KM EDA. Also, the electrostatic (ES) term in the KM scheme refers solely to the nonpolarized charge distribution, whereas our U_{el} may refer to the polarized electron distribution.

First, the binding energy for ion−water interactions is determined, keeping the charge distributions (i.e., fluctuating charges on the water and Drude position on the ion) fixed. This is equivalent to the binding energy in nonpolarizable models.

$$\Delta E_{\mathrm{np}} = U_{\mathrm{vdw}} + U_{\mathrm{repl}} + U_{\mathrm{el}} - \sum E_{\mathrm{gp}} \tag{12}$$

Here, U_{el} is due only to the ion−water interaction because the ion self- and water self-terms are the same as their isolated gas-phase values.

Next, the charge distributions are allowed to relax without CT. The charges are simultaneously equilibrated until the minimum binding energy is reached.

$$\Delta E_{\mathrm{pol}} = U_{\mathrm{vdw}} + U_{\mathrm{repl}} + U_{\mathrm{el}} + U_{\mathrm{pol,Drude}} + U_{\mathrm{pol,FQ}} - \sum E_{\mathrm{gp}} \tag{13}$$

Because the charges redistribute, the ion self, water self, and ion−water interactions are all variable.

Finally, CT is allowed. After CT, the charge distribution within the ion and water are again relaxed to find the minimum binding energy

$$\Delta E_{\mathrm{ct}} = U_{\mathrm{vdw}} + U_{\mathrm{repl}} + U_{\mathrm{el}} + U_{\mathrm{pol,Drude}} + U_{\mathrm{pol,FQ}} + U_{\mathrm{CT}} - \sum E_{\mathrm{gp}} \tag{14}$$

Again, the ion self, water self, and ion−water interactions are all variable; they are different from both the nonpolarizable and polarizable (non-CT) charge distribution.

Molecular Dynamics Simulations. Simulation details are the same as in ref 2. In-house code is used to simulate a single ion in 256 water molecules with three-dimensional periodic boundary conditions, except as noted below. The water model is TIP4P-FQ+DCT,[1] which includes charge transfer through the discrete charge transfer scheme and polarizability via the fluctuating charge method.[1,29,30] Parameters for Na^+, K^+, and Cl^- are taken from ref 2, and I^- is taken from ref 4. The rigid water bonds are constrained with SHAKE.[31] The TPN ensemble is used with T = 298 K and P = 1 atm. Charge degrees of freedom are held at 1 K. A Nosé−Hoover thermostat and Anderson barostat are used.[31] Drude particles on the ions have a mass of 0.4 amu, which is subtracted from the mass of the ion center. The Drude positions are propagated using the same method as Lamoureux and Roux.[32] Ewald summation is used to handle long-range electrostatics.[31] A 1 fs time step is used. Diffusion constants are determined via the Stokes−Einstein equation in the EVN ensemble, averaging over 50 separate 50 ps simulations with one ion and 512 water molecules.

Free Energy Calculations. Single ion free energies of hydration are calculated using thermodynamic integration (TI) following the method of Warren and Patel.[33] TI calculations are performed using separation-shifted (or soft-core) scaling in which the electrostatic and Lennard−Jones potentials are modified so that there are no singularities in the noninteracting limit.[34] The scaling is done by replacing the distance between solute and solvent atoms, r_{ij}, by $(r_{ij}^2 + (1-\lambda)\delta)^{1/2}$, where λ is the TI variable and the parameter δ is set to 7 Å^2. The TI calculations used 21 equally spaced λ values from zero to one with each simulated for 1 ns. These simulations used 512 water molecules and 1 ion with tinfoil conducting boundary conditions for the Ewald sums.

Five corrections have to be added to the TI free energy. Four of these are corrections for the finite size of the simulation box

DOI: 10.1021/ct501173n
J. Chem. Theory Comput. 2015, 11, 1658−1667

Table 2. CT in Zinc−Water Clusters

$n_i + n_o$	optimization method	basis set	r (M−O) (Å)	charge method	basis set	$q(M)$ (e)	q_{CT}/n_i (e)
1 + 0	TPSS	A	1.870	MP2	A	1.7882	0.2118
				MP2	B	1.7852	0.2148
	TPSS-GD3BJ	C	1.883	MP2	C	1.7699	0.2301
6 + 0	TPSS	C	2.105	HF	C	1.6546	0.0576
6 + 4	PBEPBE	D		HF	C	1.6100	0.0650
6 + 8	PBEPBE	D		HF	C	1.6047	0.0659
6 + 12	PBEPBE	D		PBEPBE	C	1.6115	0.0648

Table 3. CT in Magnesium−Water Clusters

$n_i + n_o$	optimization method	basis set	r (M−O) (Å)	charge method	basis set	$q(M)$ (e)	q_{CT}/n_i (e)
1 + 0	TPSS	J	1.933	MP2	J	1.9256	0.0744
6 + 0	PBE	J	2.111	HF	J	1.8374	0.0271
	TPSS		2.100	HF		1.8321	0.0280
6 + 4	PBEPBE	K		PBEPBE	L	1.8416	0.0264
6 + 8	PBEPBE	K		PBEPBE	L	1.8383	0.0270
6 + 12	PBEPBE	K		PBEPBE	L	1.8398	0.0267

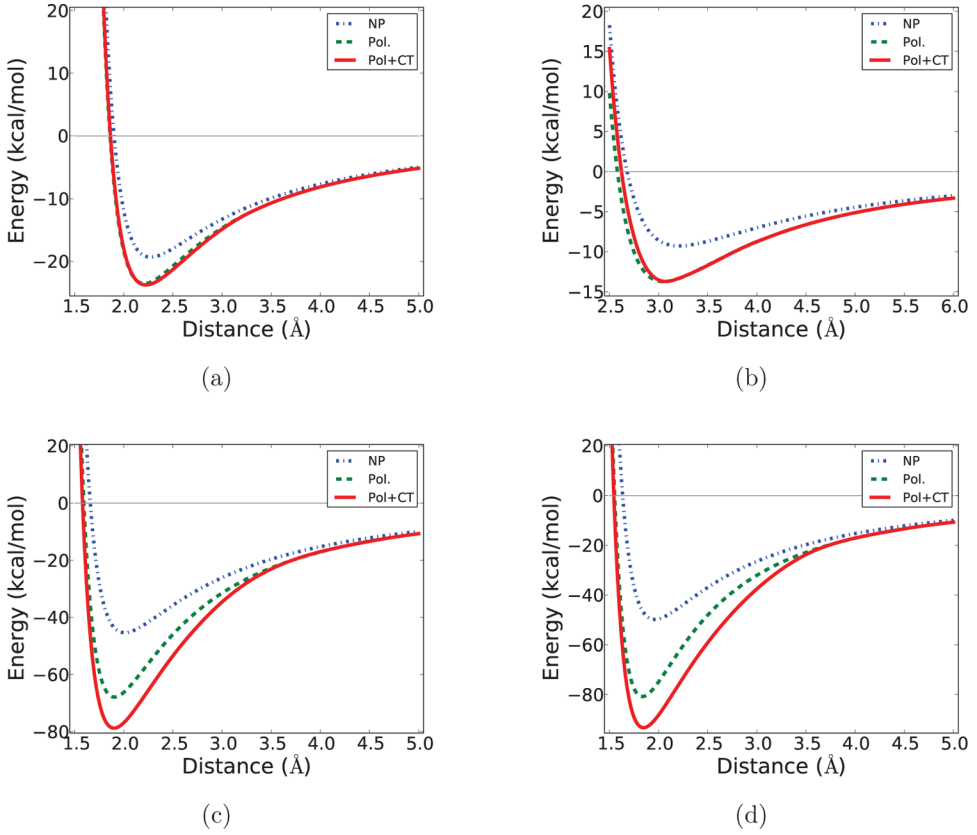

Figure 1. Comparison of ΔE_{np}, ΔE_{pol}, and ΔE_{CT} for (a) sodium, (b) chloride, (c) magnesium, and (d) zinc.

and are relatively small. The first correction is for the interaction of the ion with its periodic images using

$$\Delta G_W = \frac{q^2}{8\pi\epsilon_0\epsilon}\frac{\xi}{L} \tag{15}$$

where ϵ is the dielectric constant of the model (ϵ = 78 for TIP4P-FQ+DCT[1]), ξ is −2.837297, and L is the unit cell box length (for our simulations, L = 24.86726 Å).

Periodic interactions between the ion and solvent are corrected using

$$\Delta G_\epsilon = \frac{q^2}{6\epsilon_0 L}\left(1 - \frac{1}{\epsilon}\right)\left[\left(\frac{R_I}{L}\right)^2 - \frac{4\pi}{15}\left(\frac{R_I}{L}\right)^5\right] \tag{16}$$

where R_I is the radius of the ion, taken here to be the point where the water−ion pair correlation function first becomes nonzero (R_I = 1.90 Å for Mg^{2+} and 1.99 Å for Zn^{2+}).

A correction for the charged system term in the Ewald energy is made using

$$\Delta G_\kappa = \frac{-q^2}{8\epsilon_0\kappa^2 L^3} \tag{17}$$

DOI: 10.1021/ct501173n
J. Chem. Theory Comput. 2015, 11, 1658−1667

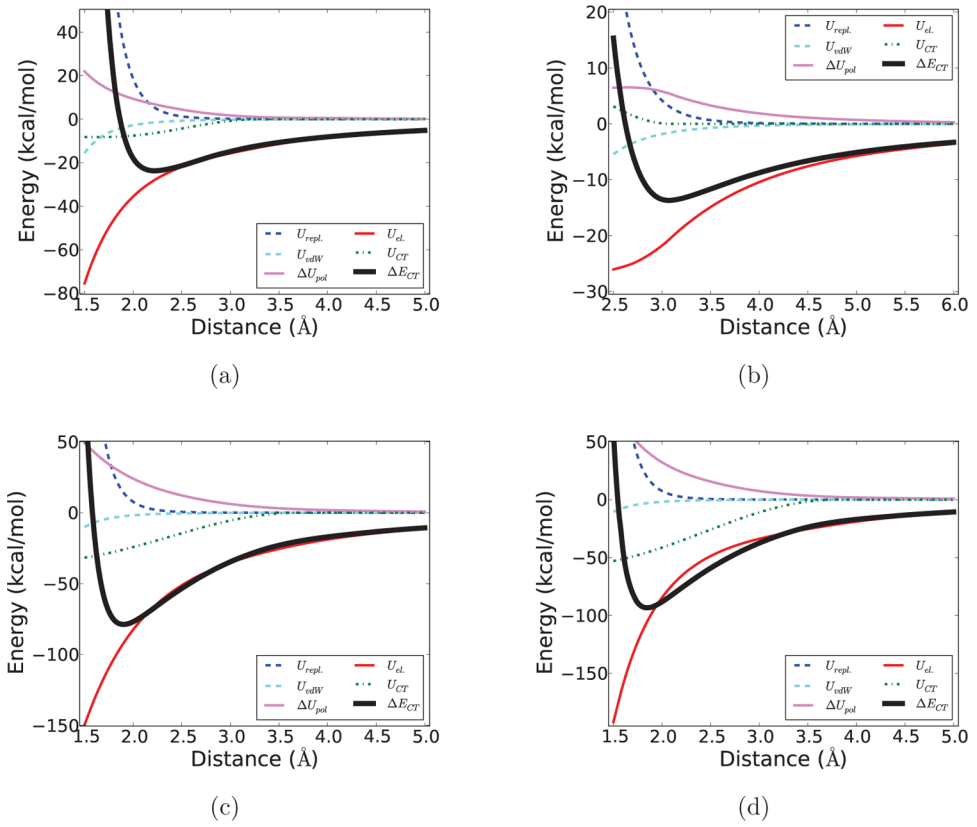

Figure 2. Decomposition of all terms in eq 1 for (a) sodium, (b) chloride, (c) magnesium, and (d) zinc.

where κ is the Ewald screening parameter. We used $\kappa = 0.34$ Å^{-1}.

A long-range correction for the Lennard–Jones ion–water interaction, U_{LJ}, is

$$\Delta G_{LRC} = 4\pi\rho \int_{r_{sw}}^{r_{cut}} U_{LJ}(r)(1 - S(r))r^2 \, dr + 4\pi\rho \int_{r_{cut}}^{\infty} U_{LJ}(r)r^2 \, dr \quad (18)$$

where ρ is the water number density, $S(r)$ is a switching function that switches off the Lennard–Jones interaction between r_{sw} and r_{cut}.

The fifth term corrects for the potential of crossing the air/liquid interface to give what is termed the "real" solvation free energy. This term is important for comparing single ion free energies to experimental values and is given by $\Delta G_\phi = q\phi$, where q is the charge of the ion and ϕ is the surface potential. In the TIP4P-FQ+DCT model, the surface potential is −0.50 V.[5]

RESULTS

Properties of Dimers and Clusters from Quantum Mechanics. Tables 2 and 3 contain the charge transfer (CT) data from quantum mechanical (QM) studies of ion–water dimers and clusters. Additional data can be found in the Supporting Information.

The ion–water distances in the dimers optimized with TPSS are consistent with high-level ab initio calculations (see Table 5). Adding dispersion corrections to the energy increases the optimal zinc–water distance by 0.013 Å, probably due to Becke–Johnson damping at short distances. Neither adding diffuse functions nor using an effective core potential (ECP) for the zinc cation alters CT. The HF electron density gives the least amount of CT, whereas DFT shows the most CT. As the ion–water distance increases, charge transfer (CT) drops off exponentially, as is seen in previous studies.[35]

The difference in the amount of CT between Zn^{2+} and Mg^{2+} has been proposed to be one source of their differing behaviors.[6] MP2 shows CT of 0.2118–0.2301 e for zinc from a single water. The CT to magnesium is about one third of that at 0.0744 e. In clusters with six or more waters, the Zn^{2+}–O_w and Mg^{2+}–O_w distances are nearly the same as their respective ion–water distances in bulk. The amount of CT per water is less when a greater number of waters coordinate the ion, which is consistent with other results (unpublished data). Comparing CT from the dimer to the six water clusters, only 33% of the dimer CT is transferred in the 6-water cluster for zinc, compared to 42% for that of magnesium. However, the total amount of CT for zinc in the cluster is still greater than that of magnesium in the cluster.

Previous studies have shown that an ion's second solvation shell does not affect CT between the ion and its first solvation shell.[2] To see whether that conclusion holds for divalent ions, we added waters to the second solvation shell of the six-water cluster. Consistent with previous results, little influence of the second solvation shell on ion charge is seen. Using a large basis set, we find that the charge of the central ion does not change no matter how many waters are in the second solvation shell. This allows us to apply our previous model, which does not have three-body CT, without modifications.

Energy Decomposition of Ion–Water Dimers. Figure 1 shows the decrease in binding energy with the addition of polarization and CT to the model. For monovalent ions, the

DOI: 10.1021/ct501173n
J. Chem. Theory Comput. 2015, 11, 1658–1667

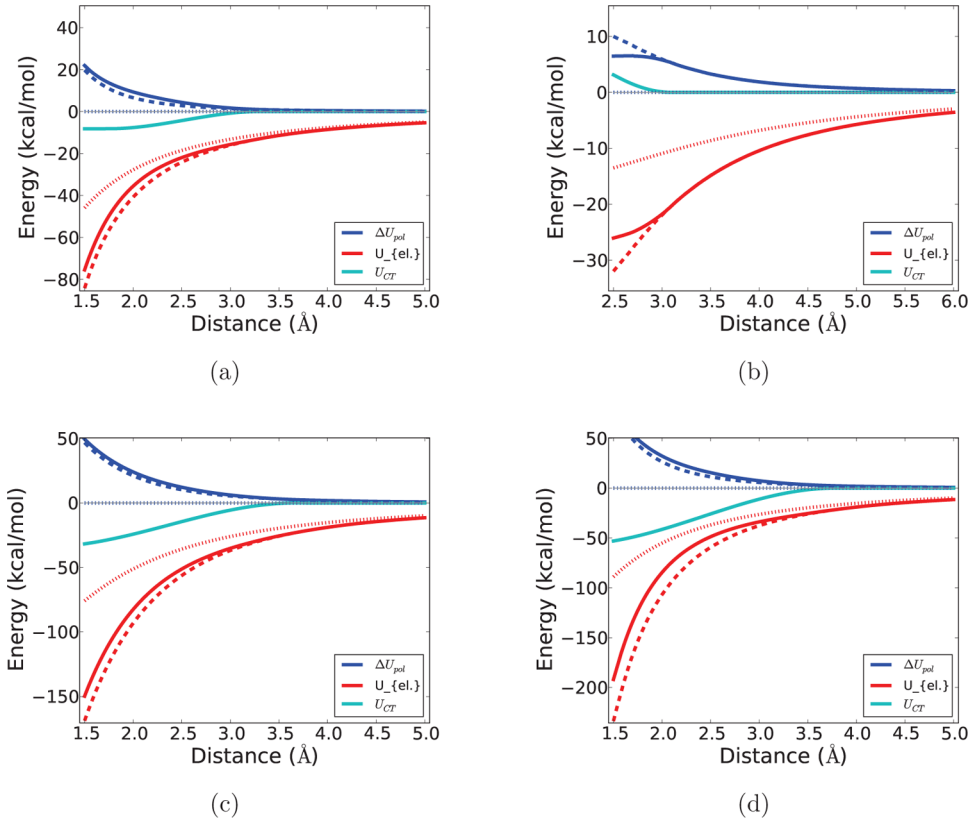

Figure 3. Comparison of changes in U_{el}, $\Delta U_{pol,Drude}$, $\Delta U_{pol,FQ}$, and U_{CT} in the nonpolarized (dotted lines), polarized (dashed lines), and polarized +CT (solid lines) models for (a) sodium, (b) chloride, (c) magnesium, and (d) zinc.

Table 4. Parameters for Divalent Cations[a]

ion	σ_{LJ} (Å)	ϵ_{LJ} (kcal mol^{-1})	q_D (e)	a_{damp} (Å)	Q_{CT} (e)	r_{CT1} (Å)	r_{CT2} (Å)	μ_{CT} (kcal mol^{-1} e^{-1})	η_{CT} (kcal mol^{-1} e^{-2})
Mg	1.88	0.0437	−0.475246	0.42	0.050	1.0	3.7	699.2	663.9
Zn	1.85	0.0556	−1.124637	0.27	0.098	1.0	3.8	620.8	332.0

[a]Abbreviations: Lennard−Jones radius (σ_{LJ}) and well depth (ϵ_{LJ}), Drude particle charge (q_D), Thole-type damping parameter (a_{damp}), maximum amount of charge transfer (Q_{CT}), cut-off distances for the charge transfer switching function (r_{CT1} and r_{CT2}), and electronegativity (μ_{CT}) and hardness (η_{CT}) for the CT energy.

main reduction in energy is due to polarization, which is on average an 18% reduction. CT results in only 2% or less further reduction. For the divalent cations, polarization results in >50% reduction in binding energy. CT further lowers the binding energy by 16%. Thus, for all of the ions, the main impetus for binding is the ion−water electrostatic interaction to which polarization contributes a significant amount. The CT contribution for divalent cations is much more significant than that for monovalent ions.

The components of eq 1 are shown in Figure 2 for the total interaction energy, including polarization and CT. Ion−water electrostatic interactions are dominant in the binding energy at distances greater than the equilibrium distance for all ions. The self-energies of polarized water and ions are combined in ΔU_{pol}. The main contribution is from the water self-term; the ion self-term is <1 kcal mol^{-1}. The self-energy ΔU_{pol} is positive, indicating that polarization increases the internal energy of water and the ion relative to the energy of the isolated gas-phase. The total binding energy ΔE_{CT} tracks $U_{repl} + U_{el-iw}$ (as long as the polarized charges are used) for all ions. It is unclear whether $\Delta E_{CT} \approx U_{repl} + U_{el-iw}$ is a general trend or is due to a fortuitous cancellation of errors for these ions.

Figure 3 shows the changes in U_{el} (ion−water interaction), ΔU_{pol}, and U_{CT} in the nonpolarizable, polarizable, and CT models. In the nonpolarizable model, the self-terms are zero, and the binding is due to the ion−water interactions. With polarization, the self-term becomes less favorable compared to the gas phase; this is called the polarization cost (i.e., the increase in self-energy due to polarization). However, with polarization, the ion−water term becomes more favorable, leading to an overall more favorable binding energy. For cations, the addition of CT leads to further cost in terms of less favorable electrostatics (increases the self-term and ion−water term). However, U_{CT} compensates for the decreased favorability of ion−water electrostatics. For anions, CT decreases the polarization cost in water, possibly due to the opposite direction of CT.

Starting with large separations, electrostatics for the non-polarizable, polarizable, and polarizable+CT cases converge, indicating the local nature of the polarization and CT interactions. Plots of these changes for potassium and iodide are contained in the Supporting Information along with plots of the Kitaura−Morokuma EDA terms.

Single-Ion Properties in Bulk Liquid Water. The parameters that best reproduce the target properties are

DOI: 10.1021/ct501173n
J. Chem. Theory Comput. 2015, 11, 1658−1667

shown in Table 4. The dimer properties produced by the parameters in Table 4 are shown in Table 5. The energies are

Table 5. Dimer Properties of Divalent Cations[a]

pair	E_{min} (kcal mol^{-1})	r_{min} (Å)	
Mg^{2+}–H_2O	−78.8	1.90	this work
	−78.8[b]	1.942[b]	target
Zn^{2+}–H_2O	−93.4	1.85	this work
	−99[c]	1.86[c]	target

[a]The results of the present MD model are compared with quantum mechanical calculations. Experimental results for E_{min} and r_{min} are given in the middle columns of the second row. [b]Analyzed with QCISD/6-311G* (properties from ref 11). [c]Analyzed with CCSD-(T)/CBS (properties from ref 13) and CCSD(T)/B2 with relativistic corrections (properties from ref 12).

consistent with high-level quantum calculations. The aqueous properties produced by the parameters in Table 4 are shown in Table 6. The target properties were derived from X-ray diffraction (XRD) and extended X-ray absorption fine structures (EXAFS) when possible. If these were not available, ab initio molecular dynamics (AIMD) were used instead. Figures of the radial distribution functions (RDF) are shown in the Supporting Information.

Solvation Shell Properties. The water charge is plotted based on the distance from the ion in Figure 4. The charge of water molecules in the first solvation shell of magnesium is close to zero, showing that CT from the second solvation shell into the first solvation shell is equal to the CT from the first shell to the ion. The first solvation shell of zinc is positive, in contrast to results for monovalent cations and magnesium. In the case of zinc, the CT from the first solvation shell to the ion is greater than the CT from the second shell to the first shell, resulting in an overall positive first solvation shell.

The charge of the ion in water is 1.61 *e* for zinc and 1.81 *e* for magnesium. The distribution of the ion charge for both is very narrow with a standard deviation of ∼0.01 *e*, indicating that the local solvation structure does not fluctuate very much and that the ion charge never gets near 2 *e*. The charge lost from the divalent cations does not stay within the first two solvation shells. The charge of the zinc in water is 1.61 *e*. The overall charge of all the molecules in the first solvation shell is 0.20 *e* and in the second is −0.01 *e*. This leaves a charge of 0.20 *e* for all of the water molecules beyond the second solvation shell. For magnesium, which has an average charge of 1.81 *e*, the first solvation shell has a charge of −0.01 *e* and the second solvation shell has a charge of ∼0, which also leaves a charge of 0.20 *e* among all of the other water molecules. Ten percent of the charge is located in the bulk for both ions, leaving 10% of the ion charge located outside the second solvation shell, which is consistent with the results for monovalent ions.[2,4]

Water molecules in the first solvation shell have a dipole moment that is enhanced relative to their bulk value of 2.6 D (see Table 6). The polarizable AMOEBA model[36] and AIMD[37,38] also find larger dipole moments for the first solvation shell. This increased dipole is in contrast to monovalent ions for which the dipole moment of the first solvation shell is a little less than or approximately equal to the bulk dipole.[2,39,40]

Free Energy Calculations. Some disagreement exists on the single ion hydration free energies, ΔG_{hydr}, of multivalent ions. The values presented by Tissandier et al.[41] are considered to be the best estimates for monovalent ions and have recently been confirmed by Coe.[42] Thus, we calculated ΔG_{hydr} of Mg^{2+} and Zn^{2+} from Tissandier et al.'s ΔG_{hydr} of Cl^- and the experimental whole salt ΔG_{hydr} of $MgCl_2$ and $ZnCl_2$. Yu et al.[43] report that ΔG_{hydr} ($MgCl_2$) = −607.0 kcal mol^{-1} and ΔG_{hydr} ($ZnCl_2$) = −637.2 kcal mol^{-1}. Tissandier et al. found that ΔG_{hydr} (Cl^-) = −72.7(2) kcal mol^{-1}. We calculated that ΔG_{hydr} (Mg^{2+}) = −461.6 kcal mol^{-1} and ΔG_{hydr} (Zn^{2+}) = −491.8 kcal mol^{-1}. These values are ∼30 kcal mol^{-1} more negative than those reported by Marcus[14] and Schmid.[44] This is consistent with Tissandier et al. who generally report cation hydration free energies that are more negative than those of Marcus and Schmid.

For the parameter sets in Table 4, the hydration free energies are ΔG_{hydr} (Mg^{2+}) = −460.9(0.2) kcal mol^{-1} and ΔG_{hydr} (Zn^{2+}) = −490.8(0.2) kcal mol^{-1}. When combined with the CT model for Cl^-, which has a single ion free energy of −73.1(0.3) kcal mol^{-1},[2] the whole salt free energies are −607.1(0.6) kcal mol^{-1} for $MgCl_2$ and −637.0(0.6) kcal mol^{-1} for $ZnCl_2$.

Kinetics. The experimental diffusion constants are 0.71 × 10^{-5} cm^2 s^{-1} for Mg^{2+} and 0.70 × 10^{-5}cm^2 s^{-1} for Zn^{2+}.[45] The model gives values that are approximately a factor of 2 less than the experimental values (Table 6), but they are in good agreement with the experimental data in that both ions diffuse at the same rate and are significantly slower than monovalent ions. Previous CT models for monovalent ions give slower diffusion constants,[2,4] as do polarizable[36] and nonpolarizable[46,47] models for divalent ions.[43]

Energy Decomposition of Single Ions in Water. The energy decomposition values for the liquid phase for Mg^{2+} and Zn^{2+} in water, as well as for pure water, are given in Table 7. The energy for Zn^{2+} is 34 kcal mol^{-1} less than that of Mg^{2+}, which closely matches the differences in the single ion free energies. The free energy difference between the two ions must mostly be due to stronger ion–water interactions with very little entropic difference. The water structure around the two

Table 6. Properties of Aqueous Divalent Cations[a]

ion	g_{max}	r_{max} (Å)	n_c	$\langle q_i \rangle$ (*e*)	$\langle \mu_i \rangle$ (D)	$\langle q_{w1ss} \rangle$ (*e*)	$\langle \mu_{w1ss} \rangle$ (D)	diff (10^{-5} cm^2 s^{-1})	
Mg	18	2.06	6.0	+1.81	0.011	−0.0015	2.93	0.34(4)	this work
Mg	14–19[b,c]	2.04[d]	6.0[d]				3.3[b]	0.70[f]	target
Zn	18	2.06	6.0	+1.61	0.067	0.033	3.01	0.35(4)	this work
Zn	17[c]	2.08[e]	6.0[g]					0.71[f]	target

[a]The properties of the radial distribution are the first maximum (g_{max}), its location (r_{max}), and the coordination number (n_c). The average charge ($\langle q_i \rangle$) and dipole ($\langle \mu_i \rangle$) of the ion and the average charge ($\langle q_{w1ss} \rangle$) and dipole ($\langle \mu_{w1ss} \rangle$) of the first solvation shell are shown. The translational diffusion constant is shown in the last data column. Numbers in parentheses indicate standard error. [b]Analyzed by AIMD (properties from refs 37 and 38). [c]Analyzed by MD (properties from ref 43). [d]Analyzed by XRD (properties from ref 53). [e]Analyzed by EXAFS (properties from ref 54). [f]Properties from ref 45. [g]Analyzed by EXAFS (properties from refs 55 and 56).

DOI: 10.1021/ct501173n
J. Chem. Theory Comput. 2015, 11, 1658–1667

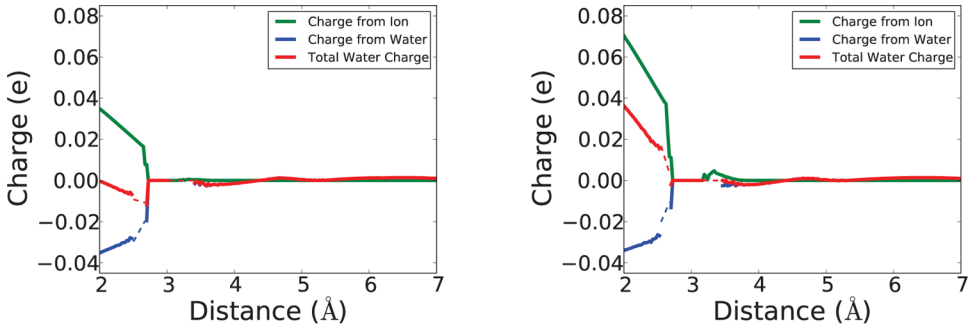

Figure 4. Total water charge in the solvation shells around (a) magnesium and (b) zinc. The contributions from the ion and other water molecules are shown. The dashed lines indicate that the data has been smoothed due to poor sampling in that region.

Table 7. Energy Decomposition for a Single Ion in Bulk and Pure Water with 256 Water Molecules and for the Ion−Water Dimers[a]

	nonpolarizable	polarizable	full
pure water	−1547(3)	−2480(4)	−2553(4)
water + Mg^{2+}	−1873(3)	−2905(4)	−3019(4)
(water + Mg^{2+})−(pure water)	−326(4)	−425(6)	−466(6)
water−Mg^{2+} dimer	−45.3	−67.9	−78.8
water + Zn^{2+}	−1891(3)	−2941(4)	−3053(4)
(water + Zn^{2+})−(pure water)	−344(4)	−461(6)	−500(6)
water−Zn^{2+} dimer	−46.6	−80.8	−93.4

[a]Numbers in parentheses indicate standard error.

ions is similar, so a similar entropy of hydration is reasonable. The nonpolarizable component is slightly more attractive for Zn^{2+}, just like it is for the dimer interaction, because the ion−water distance is slightly shorter. Polarization stabilizes Zn^{2+} more than Mg^{2+} similar to that for the dimer. The zinc ion is more polarizable, and zinc's first solvation shell water molecules also have larger dipoles (see Table 6). Charge transfer stabilizes both ions approximately the same (∼40 kcal mol^{-1}) in liquid, whereas for the dimer, charge transfer is a bigger component for zinc. The different contributions for polarization and charge transfer indicate how nonadditive effects are important for these systems. Polarization has a bigger effect on Zn^{2+} in liquid and charge transfer has a bigger effect on zinc in the gas phase compared to Mg^{2+}.

CONCLUSIONS

Models that treat both polarizability and charge transfer have been developed for Mg^{2+} and Zn^{2+}. These models reproduce the dimer pair energy and single ion hydration free energy. The energy composition analysis, as shown in Figures 3, reveals an important difference between polarization and charge transfer. Polarization requires some self-energy (ΔU_{pol}) to distort the electronic distribution on a particle, but the enhanced electrostatic interaction between the particles more than compensates (i.e., the dashed lines are more negative than the dotted lines). Charge transfer moves charge between an ion and water so that the ion's charge is smaller in magnitude and weakens the electrostatic interaction. The decreased interparticle interaction is evident in Figures 3, in which the electrostatic interaction after CT (solid line) is above the electrostatic interaction before CT (dashed line). This loss of energy is compensated for by a self-energy term (U_{CT}). This charge transfer effect is the same in ion pairs[2] and the water dimer,[1] acting to weaken interparticle interactions and driven by self-energy. Thus, both polarization and charge transfer are attractive targets (see Figure 1) but for completely different reasons.

The ions transfer a significant fraction of their charge to the solvent (0.19 *e* for Mg^{2+} and 0.39 *e* for Zn^{2+}). That charge is transferred directly to the first solvation shell (as shown with a green line in Figure 4. Because of CT between water molecules, the first solvation shell is less positive than it would be from CT of the ion alone. This results in a first solvation shell that has zero charge on average for Mg^{2+} or 0.03 *e* for Zn^{2+}. Previous work, both with CT models[2,4] and ab initio methods[48,49] for singly charged anions and cations, found a negatively charged first solvation shell. The zinc solvation shell is positive because the amount of charge transfer from water to the ion is larger than it is for the other ions, which outweighs the charge transferred from the second solvation shell. The combined charge of the six water molecules in the first solvation shell and the charge of the ion leaves a charge of 0.20 *e*, which is 10% of the ion's charge. This charge is shared among the bulk water and is not located only on the second solvation shell. Monovalent ions also give up 10% of their charge to the bulk liquid.[2] Charge transfer between water molecules in the bulk results from a slight hydrogen-bond imbalance induced by the ion. Long-range effects of ions on hydrogen bonds has been reported in studies with classical (non-CT) force fields as well.[50] Charge transfer from an ion to water was recently shown to be necessary to describe changes in water dynamics due to the addition of anions.[51]

The energy decomposition analysis, as well as previous studies of ion solvation,[2] aqueous interfaces,[4,5,52] and water dynamics[51] all suggest that charge transfer has a distinct influence on the properties of liquids and solutions. The development of models that take into account variable CT and polarization will allow for further investigation of their effects on the properties of ionic solutions.

ASSOCIATED CONTENT

Supporting Information

Tables of charge transfer data for ion−water dimers and clusters using different electronic structure methods, optimized geometries of ion−water clusters, energy partitioning results for potassium and iodide, Kitaura−Morokuma energy decomposition results, and water−ion pair correlation functions. This

DOI: 10.1021/ct501173n
J. Chem. Theory Comput. 2015, 11, 1658−1667

material is available free of charge via the Internet at http://pubs.acs.org.

AUTHOR INFORMATION

Corresponding Author

*E-mail: srick@uno.edu.

Notes

The authors declare no competing financial interest.

ACKNOWLEDGMENTS

This work was supported by the National Science Foundation (Contract CHE-0611679). This material is based upon work supported by the Louisiana Optical Network Institute (LONI) and by the National Science Foundation under the NSF EPSCoR Cooperative Agreement No. EPS-1003897 with additional support from the Louisiana Board of Regents. M.S. gratefully acknowledges support from the State of Louisiana Board of Regents.

REFERENCES

(1) Lee, A. J.; Rick, S. W. *J. Chem. Phys.* **2011**, *134*, 184507.
(2) Soniat, M.; Rick, S. W. *J. Chem. Phys.* **2012**, *137*, 044511.
(3) Bader, R. F. W. *Atoms in Molecules - A Quantum Theory*; Univerity Press: Oxford, 1990.
(4) Soniat, M.; Rick, S. W. *J. Chem. Phys.* **2014**, *140*, 184703.
(5) Wick, C. D.; Lee, A. J.; Rick, S. W. *J. Chem. Phys.* **2012**, *137*, 154701.
(6) Li, Y. L.; Mei, Y.; Zhang, D. W.; Xie, D. Q.; Zhang, J. Z. H. *J. Phys. Chem. B* **2011**, *115*, 10154−10162.
(7) Wu, J. C.; Piquemal, J.-P.; Chaudret, R.; Reinhardt, P.; Ren, P. *J. Chem. Theory Comput.* **2010**, *6*, 2059−2070.
(8) Chakravorty, D. K.; Wang, B.; Lee, C. W.; Giedroc, D. P.; Merz, K. M. *J. Am. Chem. Soc.* **2011**, *134*, 3367−3376.
(9) Tuccinardi, T.; Martinelli, A.; Nuti, E.; Carelli, P.; Balzano, F.; Uccello-Barretta, G.; Murphy, G.; Rossello, A. *Bioorg. Med. Chem.* **2006**, *14*, 4260−4276.
(10) Marcus, Y. *Chem. Rev.* **1988**, *88*, 1475−1498.
(11) Alcami, M.; Gonzalez, A. I.; Mo, O.; Yanez, M. *Chem. Phys. Lett.* **1999**, *307*, 244−252.
(12) Amin, E. A.; Truhlar, D. G. *J. Chem. Theory Comput.* **2008**, *4*, 75−85.
(13) Rayón, V. M.; Valdés, H.; Díaz, N.; Suárez, D. *J. Chem. Theory Comput.* **2008**, *4*, 243−256.
(14) Marcus, Y. *J. Chem. Soc., Faraday Trans.* **1991**, *87*, 2995−2999.
(15) Cisneros, G. A.; Karttunen, M.; Ren, P.; Sagui, C. *Chem. Rev.* **2014**, *114*, 779−814.
(16) Morokuma, K. *Acc. Chem. Res.* **1977**, *10*, 294−300.
(17) Stone, A. J. *Chem. Phys. Lett.* **1993**, *211*, 101−109.
(18) Thompson, W. H.; Hynes, J. T. *J. Am. Chem. Soc.* **2000**, *122*, 6278−6286.
(19) van der Vaart, A.; Merz, K. M., Jr. *J. Chem. Phys.* **2002**, *116*, 7380.
(20) Khaliullin, R. Z.; Bell, A. T.; Head-Gordon, M. *J. Chem. Phys.* **2008**, *128*, 184112.
(21) Stevens, W. J.; Fink, W. H. *Chem. Phys. Lett.* **1987**, *139*, 15−22.
(22) Glendening, E. D. *J. Phys. Chem. A* **2005**, *109*, 11936−11940.
(23) Tao, J.; Perdew, J. P.; Staroverov, V. N.; Scuseria, G. E. *Phys. Rev. Lett.* **2003**, *91*, 146401.
(24) Frisch, M. J.; Trucks, G. W.; Shlegel, H. B.; Scuseria, G. E.; Robb, M. A.; Cheesema, J. R.; Scalmani, G.; Barone, V.; Mennucci, B.; Petersson, G. A.; Nakatsuji, H.; Caricato, M.; Li, X.; Hratchian, H. P.; Izmaylov, A. F.; Bloino, J.; Zheng, G.; Sonnenberg, J. L.; Hada, M.; Ehara, M.; Toyota, K.; Fukuda, R.; Hasegawa, J.; Ishida, M.; Nakajim, T.; Honda, Y.; Kitao, O.; Nakai, H.; Vreven, T.; Montgomery, J. A., Jr.; Peralta, J. E.; Olgiara, F.; Bearpark, M.; Heyd, J. J.; Brothers, E.; Kudin, K. N.; Staroverov, V. N.; Kobayashi, R.; Normand, J.; Raghavachari, K.; Rendell, A.; Burant, J. C.; Iyengar, S. S.; Tomasi, J.; Cossi, M.; Rega, N.; Millam, J. M.; Klene, M.; Knox, J. E.; Cross, J. B.; Bakken, V.; Adamo, C.; Jaramillo, J.; Gomperts, R.; Stratmann, R. E.; Yazyev, O.; Austin, A. J.; Cammi, R.; Pomelli, C.; Ochterski, J. W.; Martin, R. L.; Morokuma, K.; Zakrzewski, V. G.; Voth, G. A.; Salvador, P.; Dannenberg, J. J.; Dapprich, S.; Daniels, A. D.; Farkas, O.; Foresman, J. B.; Ortiz, J. V.; Cioslowski, J.; Fox, D. J. *Gaussian 09*, revision A.1; Gaussian Inc: Wallingford, CT, 2009.
(25) Grimme, S.; Ehrlich, S.; Goerigk, L. *J. Comput. Chem.* **2011**, *32*, 1456−1465.
(26) Perdew, J. P.; Burke, K.; Ernzerhof, M. *Phys. Rev. Lett.* **1996**, *77*, 3865.
(27) Perdew, J. P.; Burke, K.; Ernzerhof, M. *Phys. Rev. Lett.* **1997**, *78*, 1396−1396.
(28) Keith, T. A. *AIMAll*, version 14.06.21; TK Gristmill Software: Overland Park, KS, 2014; aim.tkgristmill.com.
(29) Rick, S. W.; Stuart, S. J.; Berne, B. J. *J. Chem. Phys.* **1994**, *101*, 6141−6156.
(30) Olano, L. R.; Rick, S. W. *J. Comput. Chem.* **2005**, *26*, 699−707.
(31) Allen, M. P.; Tildesley, D. J. *Computer Simulation of Liquids*; Oxford Univerity: Oxford, 1987.
(32) Lamoureux, G.; Roux, B. *J. Chem. Phys.* **2003**, *119*, 3025−3039.
(33) Warren, G. L.; Patel, S. *J. Chem. Phys.* **2007**, *127*, 064509.
(34) Zacharias, M.; Straatsma, T. P.; McCammon, J. A. *J. Chem. Phys.* **1994**, *100*, 9025−9031.
(35) Belpassi, L.; Reca, M. L.; Tarantelli, F.; Roncaratti, L. F.; Pirani, F.; Cappelletti, D.; Faure, A.; Scribano, Y. *J. Am. Chem. Soc.* **2010**, *132*, 13046−13058.
(36) Jiao, D.; King, C.; Grossfield, A.; Darden, T. A.; Ren, P. *J. Phys. Chem. B* **2006**, *110*, 18553−18559.
(37) Lightstone, F. C.; Schwegler, E.; Hood, R. Q.; Gygi, F.; Galli, G. *Chem. Phys. Lett.* **2001**, *343*, 549−555.
(38) Ikeda, T.; Boero, M.; Terakura, K. *J. Chem. Phys.* **2007**, *127*, 074503.
(39) Grossfield, A. *J. Chem. Phys.* **2005**, *122*, 024506.
(40) Guàrdia, E.; Skarmoutsos, I.; Masia, M. *J. Chem. Theory Comput.* **2009**, *5*, 1449−1453.
(41) Tissandier, M. D.; Cowen, K. A.; Feng, W. Y.; Gundlach, E.; Cohen, M. H.; Earhart, A. D.; Coe, J. V.; Tuttle, T. R., Jr. *J. Phys. Chem. A* **1998**, *102*, 7787−7794.
(42) Coe, J. V. *Int. Rev. Phys. Chem.* **2001**, *20*, 33−58.
(43) Yu, H.; Whitfield, T. W.; Harder, E.; Lamoureux, G.; Anisimov, V. M.; MacKerell, A. D., Jr.; Roux, B. *J. Chem. Theory Comput.* **2010**, *6*, 774−786.
(44) Schmid, R.; Miah, A. M.; Sapunov, V. N. *Phys. Chem. Chem. Phys.* **2000**, *2*, 97−102.
(45) Haynes, W. M., Ed. *CRC Handbook of Chemistry and Physics*, 2nd ed.; CRC Press, 2014; Internet version, http://www.hbcpnetbase.com (accessed November 15, 2014).
(46) Koneshan, S.; Rasaiah, J. C.; Lyndon-Bell, R. M.; Lee, S. H. *J. Phys. Chem. B* **1998**, *102*, 4193.
(47) Guardia, E.; Sese, G.; Padro, J. A.; Kalko, S. G. *J. Solution Chem.* **1999**, *28*, 1113.
(48) Dal Peraro, M.; Raugei, S.; Carloni, P.; Klein, M. L. *ChemPhysChem* **2005**, *6*, 1715−1718.
(49) Sellner, B.; Valiev, M.; Kathmann, S. M. *J. Phys. Chem. B* **2013**, *117*, 10869−10882.
(50) Irudayam, S. J.; Henchman, R. H. *J. Chem. Phys.* **2012**, *137*, 034508.
(51) Yao, Y.; Kanai, Y.; Berkowitz, M. L. *J. Phys. Chem. Lett.* **2014**, *5*, 2711−2716.
(52) Vácha, R.; Rick, S. W.; Jungwirth, P.; de Beer, A. G. F.; de Aguiar, H. B.; Samson, J.-S.; Roke, S. *J. Am. Chem. Soc.* **2011**, *133*, 10204−10210.
(53) Caminiti, R.; Licheri, G.; Piccaluga, G.; Pinna, G. *Chem. Phys. Lett.* **1977**, *47*, 275−278.
(54) D'Angelo, P.; Benfatto, M.; Della Longa, S.; Pavel, N. V. *Phys. Rev. B* **2002**, *66*, 064209.
(55) D'Angelo, P.; Barone, V.; Chillemi, G.; Sanna, N.; Meyer-Klaucke, W.; Pavel, N. V. *J. Am. Chem. Soc.* **2002**, *124*, 1958−1967.

DOI: 10.1021/ct501173n
J. Chem. Theory Comput. 2015, 11, 1658−1667

(56) Kuzmin, S.; Obst, S.; Purans, J. *J. Phys.: Condens. Matter* **1997**, *9*, 10065.

DOI: 10.1021/ct501173n
J. Chem. Theory Comput. 2015, 11, 1658−1667